JNeurosci
THE JOURNAL OF NEUROSCIENCE

**Research Articles | Behavioral/Cognitive**

# Improving emotion control in social anxiety by targeting rhythmic brain circuits

https://doi.org/10.1523/JNEUROSCI.0769-25.2026

Received: 18 April 2025
Revised: 27 January 2026
Accepted: 25 February 2026

Copyright © 2026 the authors

*This Early Release article has been peer reviewed and accepted, but has not been through the composition and copyediting processes.The final version may differ slightly in style or formatting and will contain links to any extended data.*

**Alerts:** Sign up at www.jneurosci.org/alerts to receive customized email alerts when the fully formatted version of this article is published.

**Title:** Improving emotion control in social anxiety by targeting rhythmic brain circuits

**Abbreviated title:** Improving emotional action control in social anxiety

**Authors:** Sjoerd Meijer[1†*], Bob Bramson[1,2†], Ivan Toni[1‡], and Karin Roelofs[1,2‡]

**Affiliations:** [1]*Donders Institute for Brain, Cognition and Behavior, Centre for Cognitive Neuroimaging (DCCN), Radboud University Nijmegen, 6525 EN Nijmegen, the Netherlands.* [2]*Behavioral Science Institute (BSI), Radboud University Nijmegen, 6525 GD Nijmegen, the Netherlands.*

[*]Corresponding author. E-mail: sjoerd.meijer@donders.ru.nl

[†,‡]These authors contributed equally to this work.

**Manuscript pages:** 31

**Figures:** 4

**Tables:** 1

**Wordcount:** Abstract (166), Introduction (635), Discussion (1362)

**Key words:** social anxiety; emotion control; approach-avoidance behavior; phase-amplitude coupling; transcranial electrical brain stimulation

**Competing interests:** The authors declare that they have no competing interests.

**Acknowledgments:** We thank Jesse Lam for his support with data collection.

**Funding:** This work was funded by a consolidator grant DARE2APPROACH, from the European Research Council (ERC_CoG_772337) awarded to KR and also supporting SM and BB; by a consortium grant from the Dutch Research Council INTENSE (NWO_Crossover_17619) and by (NWO_SSH_406.20.GO.020) awarded to IT and KR.

**Data and materials availability:** All behavioral and fMRI data, along with the analysis scripts, will be made available at https://doi.org/10.34973/jjjq-nr84.

JNeurosci Accepted Manuscript

**ABSTRACT** (166/250)

Social avoidance is a hallmark of social anxiety disorder. Difficulties in controlling avoidance behavior are the core maintaining factor of this impairing condition, hampering the efficacy of existing therapies. This preregistered study tested a physiologically-grounded non-invasive enhancement of control over social approach and avoidance behavior in socially anxious individuals. Participants received dual-site phase-coupled electrical stimulation aimed at enhancing endogenous inter-regional theta-gamma phase-amplitude coupling between prefrontal and sensorimotor cortex, a mechanism known to support emotional-action control in non-anxious individuals. We measured behavioral and fMRI-BOLD responses during in-phase, anti-phase, and sham stimulations, while participants of either sex performed a social approach-avoidance task, involving either automatic or controlled emotional actions. In-phase stimulation selectively enhanced control over approach-avoidance actions. Notably, in-phase stimulation modulated neural responses in the same prefrontal region where target engagement increased as a function of trait anxiety. These findings illustrate how human neurophysiological connectivity can be leveraged to improve control over social avoidance, opening the way for mechanistically grounded clinical interventions of persistent avoidance in anxiety disorders.

**SIGNIFICANCE STATEMENT** (106/120)

Controlling automatic approach-avoid behavior is essential for human social interactions. This ability is impaired in social anxiety, and recent evidence suggests that neurotypical brains use endogenous rhythmic coupling for social emotion control. In a preregistered study, we used noninvasive electrical brain stimulation to enhance endogenous rhythmic coupling between prefrontal theta- and sensorimotor gamma-band rhythms, while highly socially anxious individuals solved an emotional control challenge. In-phase stimulation selectively enhanced emotional action control and modulated neural activity in a prefrontal cortex region where brain stimulation reactivity increased as a function of trait anxiety. These findings provide evidence for the clinical potential of this interventional approach to social anxiety.

JNeurosci Accepted Manuscript

## INTRODUCTION (635/650)

Anxiety disorders are characterized by difficulties in flexibly regulating prepotent approach and avoidance tendencies. Persistent avoidance of perceived threats contributes to the development and maintenance of anxiety by preventing extinction through exposure (Lovibond et al., 2009; Pittig et al., 2015; Craske and Stein, 2016; Rattel et al., 2017). There is an urgent need for non-invasive interventions targeted at improving emotional action control in anxious individuals. Recent work has improved cognitive and behavioral functions in neurotypical individuals, boosting inter-regional neural communication through dual-site phase-amplitude-coupled transcranial alternating current stimulation (dual-site tACS) (Polanía et al., 2012; Violante et al., 2017; Preisig et al., 2021; Grover et al., 2022). This non-invasive neuromodulation technique, grounded on the physiology of directional inter-regional neuronal communication, can also enhance emotion control in non-anxious individuals (Bramson et al., 2020a). Here, we test the translational potential of this approach by applying dual-site tACS in a group of participants selected for high social anxiety, a trait known to be associated with impaired emotional action control (Heuer et al., 2007; Roelofs et al., 2009b; van Peer et al., 2009). This translational test is a critical step toward developing clinically-relevant interventions for modulating emotional behavioral control.

Patients suffering from social anxiety disorder have particular difficulties in overriding automatic avoidance tendencies in social situations. Previous research has identified the lateral prefrontal cortex (lPFC) as a critical brain region involved in selecting between competing approach-avoidance actions (Koch et al., 2018; Bramson et al., 2020b). lPFC integrates valence signals from the amygdala with task goals to bias action competition in sensorimotor cortex (SMC) (Volman et al., 2011; Bramson et al., 2018, 2020a; Lapate et al., 2022). This functional framework is supported by causal evidence from human neuromodulation studies: perturbation of lPFC reduces accuracy on affect-incongruent trials – when prepotent emotional responses need to be overridden (Volman et al., 2011) – whereas facilitation of lPFC-SMC coupling enhances accuracy under the same demands (Bramson et al., 2020a). Human electrophysiological studies have indicated that this type of cognitive control can be implemented through rhythmic modulation of excitability in downstream areas, including the SMC and parietal cortex (Voytek et al., 2015; Bramson et al., 2018, 2020a; Weber et al., 2024). Specifically, successful control over social-emotional approach-avoidance actions has been linked to coupling between the phase of theta-band rhythms in lPFC and the amplitude of gamma-band activity in SMC (Bramson et al., 2018).

JNeurosci Accepted Manuscript

Dual-site tACS offers a means to non-invasively modulate endogenous inter-regional phase-amplitude coupling, enhancing long-range synchronization between task-relevant neural circuits (Reinhart and Nguyen, 2019; Bramson et al., 2020a; Grover et al., 2022). Our work has shown that in-phase stimulation, designed to synchronize peaks of theta-band rhythms in lPFC with the amplitude of gamma-band neural activity in SMC, improves accuracy when non-anxious participants override automatic emotional action tendencies (Bramson et al., 2020a). Notably, these behavioral improvements scaled with local target engagement: participants showing greater reductions in prefrontal BOLD during stimulation exhibited stronger behavioral facilitation. This inter-individual variation highlights the importance of considering interactions between ongoing neural activity and tACS-induced electric fields (Krause et al., 2019, 2022; Johnson et al., 2020). Furthermore, underscoring the potential of using BOLD reduction as a neural proxy for local target engagement (Bramson et al., 2020a), in line with concurrent EEG-fMRI studies showing that inhibitory low-frequency oscillations, e.g. theta, can be associated with decreased BOLD signal (Scheeringa et al., 2011; Algermissen et al., 2022).

Given the pivotal role of the lPFC and its connectivity with SMC in regulating social emotional approach-avoidance actions (Volman et al., 2011; Bramson et al., 2020a), we here used dual-site tACS over lPFC and SMC, aiming to improve emotion control in highly socially anxious individuals. Specifically, we applied in-phase and anti-phase dual-site tACS while forty-nine highly socially anxious individuals performed a social approach-avoidance task. We used concurrent fMRI to quantify prefrontal engagement during control over the emotional action tendencies.

JNeurosci Accepted Manuscript

## MATERIALS AND METHODS

### Participants

Fifty-two highly socially anxious students (39 females) from Radboud University, Nijmegen, were recruited to participate in this pre-registered experiment (https://osf.io/j9s2z/). The local ethics committee approved the experiment (METC Arnhem-Nijmegen: CMO2014/288). Two participants were excluded due to malfunctioning of the stimulation equipment, and one participant was excluded for failing to comply with task instructions during one of the stimulation sessions. Participants were selected based on high self-reported social anxiety levels, as detailed below, and screened for eligibility criteria, including no history of mental illness other than anxiety disorders or current use of psychoactive medication. Additionally, all participants had normal or corrected-to-normal vision and underwent screening for contraindications to magnetic resonance imaging (MRI) and non-invasive transcranial electrical stimulation. The mean age of participants was 24.0 years (SD = ±4.3), with an age range of 19 to 40 years.

Pre-screening was conducted using the Liebowitz Social Anxiety Scale (LSAS). Participants who scored 30 or higher (on the combined fear/anxiety and avoidance sub-scales) were included, as this cutoff provides an optimal balance between sensitivity and specificity for identifying individuals who meet the criteria for social anxiety disorder (Mennin et al., 2002). This selection criterion resulted in a normal distribution of LSAS scores within our study sample, with a mean of 64.4, a standard deviation (SD) of ±18.8, and a range from 31 to 106 (**Fig. 1A**). The trait sub-scale of the State-Trait Anxiety Inventory (STAI Y-2) was also included to assess trait anxiety, serving as an inter-individual difference marker of tACS target engagement. This is because endogenous prefrontal activation in response to the emotional action control challenge varies as a function of trait anxiety (Bramson et al., 2023).

The current study in highly socially anxious individuals was powered to replicate the main finding of our previous investigation in healthy male students (Bramson et al., 2020a) that showed tACS phase- and engagement-specific effects on emotional action control (behavioral response accuracy on incongruent *vs.* congruent trials; https://osf.io/j9s2z/). This required a sample size that allowed us to detect the previously observed significant three-way interaction between Congruency (congruent, incongruent) * tACS-phase (in-phase, anti-phase) * tACS engagement (BOLD signal in lPFC during stimulation *vs*. sham) on behavioral response accuracy (correct, incorrect): $\eta_p^2$ = 0.19 (Bramson et al., 2020a). The minimum sample size required for this study to detect an effect

JNeurosci Accepted Manuscript

of comparable magnitude is 45 participants (*a priori* sensitivity power analysis of 2x2 RM-ANCOVA: $\alpha$ = .05, power = .80, $\eta_p^2$ = 0.19; G*Power v3.1; Faul et al., 2007). Given that the current sample might be more heterogeneous due to mixed-sex and anxiety-related differences, we decided to increase our planned sample size to 50 participants.

**Procedure**

The data collection procedure took place over three separate days. On the first day, participants completed the Liebowitz Social Anxiety Scale (LSAS) and State-Trait Anxiety Inventory-Trait (STAI-trait, Y-2) questionnaires. Following this, participants underwent a series of scanning procedures, including a structural T1-weighted scan, a diffusion-weighted imaging scan (DWI, as reported in Bramson et al., 2020a, 2023), and a magnetic spectroscopy scan (MRS, as reported in Bramson et al., 2020a, 2023).

On the second and third days of the experiment, neuronavigation was employed to position the electrodes over the sensorimotor cortex (SMC) and lateral prefrontal cortex (lPFC). Detailed information on electrode placement is provided in the following section. During both stimulation sessions, participants were positioned inside the MR scanner, where they first completed a 5-minute practice task. After the practice session, participants proceeded with the approach-avoidance task, which was conducted concurrently with dual-site tACS intervention and task-based functional MRI for approximately 35 minutes.

**Approach-avoidance task**

Emotional action control was manipulated using a validated social approach-avoidance task in which cognitive control is associated with lPFC-SMC theta-gamma coupling (Bramson et al., 2018), and is sensitive to the phase-dependent effects of dual-site theta-gamma phase-amplitude tACS when controlling for inter-individual variation in prefrontal BOLD response to tACS (Bramson et al., 2020a). During functional MR scanning, participants lay inside the MR scanner with a joystick in their right hand resting on their lower abdomen. Participants were instructed to approach or avoid by moving the joystick toward or away from themselves, respectively. During the task, participants received written instructions on the screen (>10 s) at the start of each block of 12 trials (~60 s) that stated, *"Pull the joystick toward yourself when you see a happy face and push away from yourself when you see an angry face"* (congruent condition), *"Push the joystick away from yourself when you see a happy face and pull toward yourself when you see an angry face"*

JNeurosci Accepted Manuscript

(incongruent condition). Congruent and incongruent conditions alternated between blocks in a pseudo-random fashion. Between blocks, there was an inter-block interval of >20 s. Each trial started with a fixation cross (500 ms) followed by a face stimulus (100 ms) to which participants had to respond within 2 s. Joystick movements over 30% of the maximum movement range were considered valid responses. If a participant did not respond, they would receive on-screen feedback stating, *"You did not move the joystick far enough"*. Instructions and the inter-block interval lead to an ~30 s wash-out period between stimulation conditions. Each participant had 288 trials on each of the two testing days, yielding 576 observations (trials) in total, equally distributed over congruency (congruent, incongruent) and stimulation (in-phase, anti-phase, sham) condition combinations (96 trials per bin).

**Dual-site tACS stimulation**

Dual-site tACS was applied online during task performance inside the MRI scanner using two sets of concentric ring electrodes (inner disc: 25 mm ø; outer ring: 80 mm inner-ø, 100 mm outer-ø) (Saturnino et al., 2017). Current direction alternated (-1 mA to +1 mA) between each disc-ring electrode set to achieve a time-varying electrical field in theta-band (6 Hz) frequency over right-lPFC and gamma-band (75 Hz) tapered with a 6 Hz theta wave over left-SMC. The tACS-phase manipulation was achieved by phase-locking gamma-band power to peaks (in-phase) or troughs (anti-phase) of the theta-band signal. This stimulation protocol was informed by prior magnetoencephalography (MEG) findings showing that emotional action control engages theta-gamma phase-amplitude coupling between lPFC and SMC during the same task (Bramson et al., 2018), and its application has previously been shown to facilitate emotional action control in non-anxious males (Bramson et al., 2020a). During sham blocks, there was an initial 10 s period of stimulation to match potential sensations related to the onset of stimulation, after which stimulation was terminated. Within a session, participants received all stimulation conditions (in-phase, anti-phase, sham) alternating in a pseudo-random fashion between stimulus blocks of 12 trials (~60 s), interleaved with periods of no stimulation (instructions between blocks; > 30 s), and never repeating the same stimulation condition for two consecutive blocks.

We used neuronavigation (Localite TMS Navigator; RRID: SCR_016126) for individualized targeting of left-SMC (MNI [-28, -32, 64] (Bramson et al., 2018, 2020a) and right-lPFC (MNI [26, 54, 0] (Neubert et al., 2014; Bramson et al., 2018, 2020a)) based on anatomical masks of regions of interest registered to individual T1-weighted scans acquired during the first session. After localization, electrodes were attached to the participant's scalp using Ten20 conductive paste (MedCaT). Inside the MR scanner, stimulation was delivered using two Neuroconn DC-Stimulator

JNeurosci Accepted Manuscript

Plus stimulators (neuroConn; impedance < 10 kOhm; RRID: SCR_015520). Stimulators were placed inside a magnetically shielded box designed with electronics that filtered out RF pulses of the MR scanner and combined with a BrainAmp ExG MR amplifier (www.brainproducts.com) that allowed continuous monitoring of stimulation output during the session.

**Modeling of stimulation currents**

The electric field magnitude (mV/mm) at the cortical target sites was estimated using SimNIBS (version 4.0; Thielscher et al., 2015). The concentric ring electrode sets were modeled as the disc (25 mm ø) and outer ring electrode (80 mm inner-ø, 100 mm outer-ø) with the same center, using a 2-layer medium (2 mm silicone rubber on top of 2 mm saline gel). The electrode sets were positioned over lPFC and SMC using the template head mesh of SimNIBS. For all media, we used standard conductivities provided by SimNIBS. Direct currents of 1 mA were modeled to flow between the center disc electrode and the outer ring. The model results of the electric field magnitude at the cortical surface for both target sites are shown in **Fig. 2A**.

**MRI**

All participants underwent magnetic resonance imaging using a 3T MAGNETRON Prisma MR scanner (Siemens AG, Healthcare Sector, Erlangen, Germany), which has a 64-channel head coil with a top opening that allows the tACS electrode wires to be routed out of the back of the scanner bore. The scans obtained during the MR sessions were aligned with a standard brain atlas to guarantee a uniform field of view (FoV) throughout the days. Each scanning day involved taking around 1800 functional images using a multi-band six sequence, 2 mm isotropic voxel size, TR/TE = 1000 / 34 ms, flip angle = 60°, phase angle P >> A, including ten volumes with reversed phase encoding direction (A >> P) used to correct image distortions.

High-resolution structural images were acquired with a single-shot MPRAGE sequence using a GRAPPA acceleration factor of 2, TR/TE = 2400/2.13 ms, an effective voxel size of 1 mm isotropic, 176 sagittal slices, a distance factor of 50%, a flip angle of 8°, orientation A >> P, and a FoV of 256 mm.

**Behavior analyses**

JNeurosci Accepted Manuscript

To examine effects of congruency (congruent, incongruent) and stimulation (in-phase, anti-phase, sham) on behavioral response accuracy (correct, incorrect), we employed mixed-effects logistic regression using the *lme4* package in R (Bates et al., 2015). The models accounted for inter-individual variability by incorporating random slopes, intercepts, and correlations across participants to adhere to the maximal random effects structure. Outputs of these models are log odds ('*b*'). Effect sizes were reported as odds ratios (ORs) with 95% confidence intervals (CIs). Statistical significance for all analyses were evaluated at the $\alpha < 0.05$ criterion.

Mixed-effects logistic regression models included behavioral accuracy (correct, incorrect) as dependent variable, with the relevant experimental conditions (Congruency, Stimulation) and their interactions as predictors (**Fig. 1C**). The tACS-engagement metric (see below; continuous variable; *Z*-scored; **Fig. 3A**) or STAI trait score (continuous variable; *Z*-scored; **Fig. 3B**) was added as a covariate to the interaction.

We hypothesized that the congruency effect in error rates would decrease for in-phase tACS and that the size of the effect per participant would depend on the BOLD effect of tACS *vs*. sham, a measure of target engagement that is orthogonal to the contrast of interest (in-phase *vs*. anti-phase). These expectations were preregistered at the Open Science Framework: (https://osf.io/j9s2z/).

To examine potential engagement-independent effects of in-phase *vs.* anti-phase tACS on mean error rates (tACS > sham), we employed a linear mixed-effects model with tACS-phase (in-phase, anti-phase) and Congruency (congruent, incongruent) as within-subject factors (**Fig. 3C**).

We explored the relationship between congruency-related amygdala modulation (BOLD: incongruent > congruent) and behavioral control (error rate: incongruent − congruent). Spearman correlations assessed whether stronger amygdala modulation was associated with better emotional action control within each tACS-phase condition (**Fig. 4A**). To test whether this amygdala-behavior relationship was modulated by target engagement differently across tACS-phase conditions, we fitted a linear mixed-effects model with amygdala modulation (continuous, Z-scored), target engagement (continuous, Z-scored), and tACS-phase (in-phase, anti-phase) as predictors of the behavioral congruency effect. The three-way interaction (amygdala × engagement × tACS-phase) tested whether the engagement-dependent modulation of amygdala-

JNeurosci Accepted Manuscript

behavior coupling differed between stimulation phases (**Fig. 4B**). Simple slopes were estimated at low (−1 SD), mean, and high (+1 SD) levels of target engagement.

**ROI masks**

The sensorimotor cortex (SMC) mask was created as a 10 mm spherical ROI centered at MNI coordinates [-36, -30, 72], based on model-based estimates of current density distribution under the SMC electrode location, along with the anatomical location used for neuronavigation. The dorsolateral prefrontal cortex (dlPFC) mask was derived from the right middle frontal gyrus mask in the probabilistic Harvard-Oxford Atlas (included in FSL). The FPl mask was derived from the Neubert probabilistic connectivity-based parcellation (Neubert et al., 2014). The bilateral amygdala mask was created using the right and left amygdala masks from the Harvard-Oxford Atlas, thresholded at 25%. The primary visual cortex (V1) mask was created as an 8 mm spherical ROI and centered at the maximum probability of V1 (MNI coordinates [-9, -96, 2]) in the Juelich Histological Atlas (included in FSL).

**fMRI analyses – preprocessing**

All image processing was performed using MELODIC 3.00, as implemented in FSL 6.0.0 (https://fsl.fmrib.ox.ac.uk; Jenkinson et al., 2012). Motion correction was applied using MCFLIRT (Jenkinson et al., 2002), while magnetic field distortions were corrected with TOPUP (Andersson et al., 2003). Functional images were rigid-body registered to the brain-extracted structural image using FLIRT (Jenkinson et al., 2002). Nonlinear registration to MNI 2 mm standard space was performed with FNIRT. Images were then spatially smoothed with a 5 mm Gaussian kernel, high-pass filtered at 100 s, and pre-whitened. Independent component analysis (ICA) was conducted with a maximum of 100 components (Beckmann and Smith, 2004), which were manually inspected to remove potential noise sources (Griffanti et al., 2017).

**fMRI analyses – GLM**

Emotional action control effects on whole-brain BOLD activation were estimated by contrasting incongruent trials (approach angry and avoid happy) with congruent trials (avoid angry and approach happy) across all stimulation conditions (in-phase, anti-phase, and sham).

*Subject-level analyses*

JNeurosci Accepted Manuscript

First- and second-level GLM analyses were performed in FSL 6.0.5 using FEAT (Jenkinson et al., 2012). At the first level, the model included 12 task regressors: approach angry, approach happy, avoid angry, and avoid happy, modeled separately for each tACS condition (in-phase, anti-phase, and sham). Each regressor covered the time interval from stimulus presentation until joystick movement onset. The model also included nuisance regressors for estimated head motion (six translation and rotation parameters), their temporal derivatives, and global signal time series from white matter and cerebrospinal fluid. First-level models from two separate stimulation sessions were combined using fixed effects analysis in FEAT (Jenkinson et al., 2012).

*Group-level analyses*

At the group level, effects were assessed using FLAME 1 with outlier de-weighting (Woolrich, 2008). Family-wise error correction was applied using cluster-based inference with a cluster-forming threshold of $|Z| > 2.3$, which provides a false error rate of approximately 5% when using FLAME 1 (Eklund et al., 2016).

*Individual estimates of tACS target engagement*

Because tACS intensity was held constant across participants, individual differences in physiological impact are expected to arise primarily from variability in head anatomy and in the interaction between the induced electric field and ongoing neural activity (Opitz et al., 2015; Krause et al., 2019, 2022; Johnson et al., 2020). Accordingly, we operationalized individual differences in stimulation impact using a measure of tACS target engagement.

Specifically, tACS-engagement effects on the whole-brain BOLD signal were assessed by comparing stimulation conditions (in-phase and anti-phase) to sham across both congruency conditions (**Fig. 1D**). To capture the net neural consequences of this interaction, we use the term 'tACS-engagement' to refer to individual variability in target engagement, as indexed by stimulation-related BOLD signal change. This measure captures inter-individual differences in how the induced electrical field interacts with local neural activity, and has previously been validated as a marker of behavioral responsiveness to dual-site tACS (Bramson et al., 2020a). Individual estimates of prefrontal tACS engagement were extracted from the 98% peak-activated voxel within the Harvard-Oxford middle frontal gyrus (dlPFC) mask. This tACS-engagement metric (active tACS > sham tACS) is orthogonal to both the tACS-phase manipulation and the emotional action control contrast.

JNeurosci Accepted Manuscript

Because concurrent fMRI-EEG studies have shown that low-frequency brain rhythms (e.g. theta) are associated with reduced BOLD signal (Scheeringa et al., 2011; Algermissen et al., 2022), in line with their predominantly inhibitory role (Yu et al., 2023; Leung and Yim, 2025), we consider a net reduction in prefrontal BOLD signal as a marker of stronger tACS engagement (see also Bramson et al., 2020a).

To validate the orthogonality of the tACS-engagement metric, we confirmed that it was uncorrelated with the contrast between in-phase > sham and anti-phase >sham (Spearman's $\rho_{(46)}$ = -0.05, $p$ = 0.7460). Moreover, both in-phase > sham and anti-phase > sham contrasts explained comparable variance in the tACS-engagement metric ($\rho_{(46)}$ = 0.73 and 0.68, respectively, both $p$ < 0.0001). One participant was excluded from this analysis due to an extreme in-phase > sham value ($|Z| > 3$).

An exploratory whole-brain correlation analysis was also conducted to examine the relationship between individual variation in STAI trait anxiety (*Z*-scored) and the tACS-engagement contrast (**Fig. 3B**).

*tACS-phase effects on dlPFC-SMC coupling*

tACS-phase effects on congruency-related changes in dlPFC coupling were examined using generalized psychophysiological interaction (gPPI) analysis (O'Reilly et al., 2012). We created an interaction contrast between congruency (incongruent > congruent), tACS-phase (in-phase > anti-phase), and the mean dlPFC BOLD time series. The mean dlPFC signal for the seed regressor was extracted from a spherical ROI with a 5 mm radius, centered at each individual's peak tACS-engagement location.

tACS-phase effects on temporal BOLD signal coupling between dlPFC (seed) and SMC (target) were assessed using both cluster-based small volume correction (**Fig. 2C**) and ROI-based analyses. Cluster-based inference was performed using Gaussian Random Field Theory correction, as implemented in FSL's cluster tool (Smith and Nichols, 2009). A cluster-defining threshold of $|Z| = 2.3$ and a corrected cluster significance threshold of $p < 0.05$ were applied to control for multiple comparisons within the ROI. ROI-based inference was performed by extracting

JNeurosci Accepted Manuscript

the PPI betas from left SMC and V1 using Featquery. V1 served as a negative control to evaluate the specificity of effects, since it is not part of the emotional action control network and was not targeted by tACS. One-tailed t-tests assessed whether dlPFC–SMC and dlPFC–V1 coupling significantly differed from zero.

*tACS-phase and congruency-dependent modulation of amygdala activation*

We conducted ROI-based analyses to evaluate how amygdala responses were modulated by tACS-phase and congruency, independently of tACS engagement. Mean BOLD parameter estimates were extracted from bilateral amygdala ROIs across the four active stimulation conditions (in-phase/congruent, in-phase/incongruent, anti-phase/congruent, anti-phase/incongruent) and analyzed using a linear mixed-effects model with tACS-phase (in-phase, anti-phase) and Congruency (congruent, incongruent) as within-subject factors, **Fig. 3D**.

*Gender-related control analysis*

To assess gender-related differences in prefrontal engagement, we extracted mean activation values corresponding to the congruency contrast (incongruent > congruent) within two prefrontal ROIs: dlPFC (based on the congruency-related activation cluster) and FPl (Neubert et al., 2014). These values were analyzed using a linear mixed-effects model with Region (FPl, dlPFC) as within-subject factor and Gender (female, male) as between-subjects factor.

JNeurosci Accepted Manuscript

## RESULTS

### Behavioral cost of emotional action control

Forty-nine participants, selected on high self-reported daily-life social anxiety (**Fig. 1A**), were instructed to use a joystick to approach happy and avoid angry faces (affect-congruent condition) or avoid happy and approach angry faces (affect-incongruent condition), **Fig. 1B**. The affect-incongruent condition requires participants to override automatic emotional action tendencies to avoid angry and approach happy faces (Roelofs et al., 2009a; Phaf et al., 2014). Expected congruency effects were observed in the baseline sham-tACS condition, with higher error rates for incongruent as compared to congruent responses ($b_{congruency}$ = 0.35, 95% *Confidence Interval* (*CI*) [0.09, 0.62], $\chi^2_{(1)}$ = 7.06, $p$ = 0.0079) (Volman et al., 2011; Bramson et al., 2018, 2020a; Kaldewaij et al., 2021), **Fig. 1C**. Specifically, the odds of participants making an incorrect response were 42% higher in the incongruent as compared to congruent condition (*Odds Ratio* (*OR*) = 1.42, 95% *CI* [1.10, 1.85]). This shows that exerting emotional action control is behaviorally costly.

### Socially anxious individuals recruit dlPFC for emotional action control

The patterns of whole-brain neural activation largely aligned with previous findings using the same task in non-anxious individuals, showing increased activation during incongruent *vs*. congruent trials in bilateral precuneus [14, -70, 36], lingual gyrus [16, -74, -4], and right dorsal anterior cingulate cortex [8, 32, 28], as well as decreased activity in bilateral medial [-8, 34, -14] and lateral orbitofrontal cortex [-40, 28, -14; 24, 28, -14], temporal pole [-42, 16, -36], fusiform cortex [40, -42, -18], amygdala [38, -4, -20], extending into hippocampus and parahippocampal gyrus (Volman et al., 2011; Bramson et al., 2018, 2020a), **Table 1** and **Fig. 1D**. However, highly anxious individuals exhibited more robust activation for incongruent trials in the dorsolateral prefrontal cortex (dlPFC; Brodmann areas 9/46d) [30, 36, 38], rather than in the lateral frontal pole (FPl) region previously found in non-anxious individuals (Bramson et al., 2020a; Kaldewaij et al., 2021; Lapate et al., 2022). The differences in emotional action control circuits between high-anxious and non-anxious individuals have been detailed in a separate paper (Bramson et al., 2023). These findings indicate that high-anxious individuals likely implement control using dlPFC rather than FPl as non-anxious individuals (Bramson et al., 2023).

### In-phase tACS strengthens dlPFC-SMC functional coupling

JNeurosci Accepted Manuscript

We used simultaneous tACS and fMRI to verify neural consequences of the tACS-phase manipulation, **Fig. 2A**. In-phase *vs.* anti-phase tACS (**Fig. 2B**) selectively enhanced functional connectivity between dlPFC and SMC target regions under the congruency challenge, as quantified using generalized psychophysiological interaction (gPPI) analysis (SMC cluster: $Z_{max}$ = 3.2, $p_{fwe}$ = 0.0184, MNI[-36, -26, 68]), **Fig. 2C**. To assess the anatomical specificity of this effect, we tested whether functional coupling between dlPFC and a non-targeted region, V1, was modulated by the tACS-phase manipulation. We observed no change in dlPFC-V1 coupling ($p$ > 0.05), supporting the network specificity of the dlPFC-SMC effect. ROI-based analyses further corroborated this: across participants, dlPFC-SMC coupling was significantly greater than zero ($t_{(48)}$ = 2.17, $p$ = 0.0173), whereas dlPFC-V1 coupling was not ($t_{(48)}$ = 0.87, $p$ = 0.1954). Together, these results demonstrate the specificity of the in-phase tACS manipulation in strengthening inter-regional dlPFC-SMC coupling.

**Facilitation of emotional action control scales with dlPFC target engagement**

Concurrent tACS-fMRI was used to study the underlying mechanisms of dual-site tACS effects, as well as to explain inter-individual variance in facilitation of behavioral performance depending on prefrontal stimulation reactivity. Following our pre-registered analysis pipeline (https://osf.io/j9s2z), we evaluated the cerebral effects of prefrontal tACS by examining BOLD activity in the region involved in implementing emotional action control in these high-anxious participants. Given that high-anxious individuals recruit dlPFC to solve emotional action control (Bramson et al., 2023), and that the dual-site tACS montage of this study evokes electrical fields covering dlPFC, we choose dlPFC BOLD activity as a metric of tACS engagement. As in (Bramson et al., 2020a), the tACS-engagement metric is obtained from a BOLD contrast (active tACS > sham tACS) that is orthogonal to both the tACS-phase manipulation and the emotional action control contrast. Here, "tACS engagement" reflects individual variability in stimulation-related BOLD signal change. In line with prior EEG–fMRI work showing that increases in low-frequency oscillatory power (e.g., theta) are often associated with reductions in BOLD signal (Scheeringa et al., 2011; Algermissen et al., 2022), we interpret a greater reduction in prefrontal BOLD during stimulation as reflecting stronger physiological engagement by tACS ("higher engagement"). This rationale has been validated in our previous study (Bramson et al., 2020a), where participants with stronger BOLD reductions during stimulation also showed larger behavioral benefits. Critically, we observe tACS-engagement and tACS-phase specific enhancement of emotional action control ($b_{dlPFC\text{-}engagement}$ = -0.34, 95% CI [-0.66, -0.02], $\chi^2_{(1)}$ = 4.43, $p$ = 0.0353), **Fig. 3A**. Participants with a more robust inhibitory response to prefrontal tACS exhibited greater improvement in emotional action control when receiving in-phase as opposed to anti-phase tACS. Planned post-hoc analyses on congruency-related error rates confirm significant engagement-dependent effects for the in-phase

JNeurosci Accepted Manuscript

(Spearman's $\rho_{(47)}$ = 0.37, $p$ = .0092) but not for the anti-phase condition (Spearman's $\rho_{(47)}$ = -0.09, $p$ = .5194). The direction and magnitude of the dual-site in-phase tACS intervention effects align with our previous report (Bramson et al., 2020a), and were specifically linked to tACS engagement measured over dlPFC. Namely, when extracting tACS engagement from FPl, a region previously reported to be decoupled from emotional action control in high-anxious individuals (Bramson et al., 2023), no significant tACS-induced changes in emotional action control were observed ($b_{FPl\text{-}engagement}$ = -0.12, 95% CI [-0.46, 0.22], $\chi^2_{(1)}$ = 0.49, $p$ = 0.4844).

Further exploration of brain-symptoms correlations revealed a positive association between higher trait anxiety levels and stronger tACS engagement in dlPFC, **Fig. 3B**. However, replacing dlPFC target engagement with trait anxiety in the model did not yield a significant effect ($b_{STAI\_trait}$ = 0.01, 95% CI [-0.03, 0.04], $\chi^2_{(1)}$ = 0.12, $p$ = 0.7310), suggesting that dlPFC target engagement captures unique variance in the behavioral effects of the tACS intervention that is not accounted for by trait anxiety alone. In summary, the findings demonstrate that dual-site tACS can effectively enhance emotional action control in high-anxious individuals by targeting phase-amplitude coupling between dlPFC and SMC.

**In-phase tACS improves valence-based action selection**

We also examined tACS-phase effects independent of individual differences in target engagement. In-phase tACS, but not anti-phase tACS, results in a general behavioral performance enhancement compared to sham ($b_{tACS\text{-}phase}$ = -0.16, $SE$ = 0.08, $p$ = 0.0403), **Fig. 3C**. Specifically, in-phase tACS reduces the odds of participants making an incorrect response by 22% across both congruency conditions compared to sham ($b_{in\text{-}phase}$ = -0.25, 95% $CI$ = [-0.39, -0.11], $p$ = 0.0004; $OR$ = 0.78, 95% $CI$ = [0.67, 0.89]). In contrast, anti-phase tACS had no significant effect on behavioral accuracy ($b_{anti\text{-}phase}$ = -0.10, 95% $CI$ = [-0.25, 0.06], $p$ = 0.2225). Consistent with our previous work (Bramson et al., 2020a), when individual differences in neural responsiveness to tACS were not controlled for, tACS-phase did not show a congruency-specific effect on performance ($\chi^2_{(2)}$ = 0.85, $p$ = 0.6548).

Next, we explored the neural mechanisms underlying the general improvement in valence-based action selection during in-phase tACS, independent of individual target engagement effects. Given prior evidence that emotion control involves amygdala dampening (Volman et al., 2011, 2013, 2016) and that suppression of task-irrelevant valence signals reduces amygdala engagement (Anticevic et al., 2010; Kanske et al., 2011; Cohen et al., 2016) we focused on

JNeurosci Accepted Manuscript

amygdala activation (bilateral). We found a significant interaction effect of tACS-phase on congruency-dependent amygdala modulation ($b_{congruency:tACS\text{-}phase}$ = 0.05, 95% CI = [0.00, 0.09], $F_{(1, 96)}$ = 4.62, $p$ = 0.0341, $\eta_p^2$ = 0.05), **Fig. 3D**. Post-hoc analyses revealed that in-phase tACS resulted in stronger congruency-related modulation of amygdala activation ($b_{congruency}$ = 0.06, $t_{(95)}$ = 3.47, $p$ = 0.0008) compared to anti-phase tACS, which showed no significant effect ($b_{congruency}$ = 0.01, $t_{(95)}$ = 0.62, $p$ = 0.5355).

**Potential mechanisms of tACS phase-dependent amygdala modulation**

In-phase tACS enhanced congruency-related amygdala modulation compared to anti-phase, despite both conditions applying identical stimulation to dlPFC. If dlPFC receives identical stimulation in both phases, why would altering the phase relationship at SMC differentially affect amygdala responses? One explanation is that potential phase-related differences in electric field strength or spatial distribution at dlPFC result in differential dlPFC efficacy in controlling the amygdala between phases. Modeling analyses showed highly comparable electric fields between tACS-phases (in-phase *vs.* anti-phase: Δ mean = +0.004 ± 0.002 mV/mm, spatial $r$ = 0.998), making this explanation unlikely. A second explanation is that in-phase tACS strengthens dlPFC-amygdala functional coupling through a network-level change in control state, improving the capacity for direct top-down regulation. However, we found no phase-dependent differences in dlPFC-amygdala connectivity during the congruency challenge ($p$ > 0.05).

A third possibility is that the amygdala responses were modulated by the state of the dlPFC-SMC circuit. At the mechanistic level, the phase manipulation at SMC does not directly alter dlPFC stimulation but rather modulates the temporal alignment of dlPFC theta peaks with gamma-band activity in SMC, specifically facilitating directional communication from dlPFC to SMC (Canolty and Knight, 2010; Voytek et al., 2015). Although amygdala receives relatively sparse direct projections from dlPFC (Petrides and Pandya, 1999), it maintains robust reciprocal connections with premotor and sensorimotor regions involved in action preparation (Amaral and Price, 1984; Ghashghaei et al., 2007; Morecraft et al., 2007). In-phase facilitation of dlPFC-SMC coupling may therefore strengthen goal-directed control pathways that compete with amygdala-driven action tendencies, downregulating valence-based signals for action selection. To empirically validate this possibility, we first confirmed that amygdala modulation related to behavioral control in both tACS-phase conditions (anti-phase: Spearman's $\rho_{(47)}$ = -0.30, $p$ = 0.0400; in-phase: Spearman's $\rho_{(47)}$ = -0.32, $p$ = 0.0277), **Fig. 4A**. We then conducted exploratory analyses to test whether this coupling varied with target engagement across phases. The coupling between amygdala modulation and behavioral control varied with target engagement differently across tACS-phase conditions (three-

JNeurosci Accepted Manuscript

way interaction: $b$ = 0.34, 95% CI [0.03, 0.64], $F_{(1, 78)}$ = 4.63, $p$ = 0.0330, $\eta_p^2$ = 0.06), **Fig. 4B**. In-phase stimulation showed a significant amygdala × engagement interaction ($b$ = 0.29, 95% CI [0.04, 0.54], $F_{(1, 45)}$ = 5.19, $p$ = 0.0240, $\eta_p^2$ = 0.11), such that the relationship between amygdala modulation and behavioral control weakened as target engagement increased. Phase differences in slope strength increased systematically across engagement levels: at low (-1 SD) and mean engagement, slopes did not differ between conditions (low: $p$ = 0.4694; mean: $p$ = 0.1930); whereas at high engagement (+1 SD), slopes diverged significantly ($b$ = -0.53, $t_{(78)}$ = -2.37, $p$ = 0.0188). Thus, we find the largest effect in individuals showing strongest tACS target engagement. As expected, anti-phase stimulation showed no such modulation by engagement; the relationship between amygdala modulation and behavioral control remained stable across all target engagement levels ($b$ = -0.03, $F_{(1, 45)}$ = 0.32, $p$ = 0.5723). These findings indicate that in-phase tACS facilitation of dlPFC-SMC coupling may reduce amygdala influence on action selection by strengthening goal-directed cortical control rather than enhancing direct dlPFC regulation of the amygdala.

**Gender does not explain shift in FPl *vs.* dlPFC recruitment for emotion control**

Given that the current study sample includes both females and males (f/m: 38/11), whereas our previous study included only male participants (Bramson et al., 2020a), we assessed potential gender-related differences in recruitment of FPl *vs.* dlPFC during emotional action control. This analysis revealed no significant interaction (Region × Gender: $F_{(1, 47)}$ = 0.89, $p$ = 0.3501), providing no evidence for gender-related differences in FPl vs. dlPFC recruitment. This finding is consistent with previous research using a similar approach-avoidance task in a mixed-gender sample (f/m: 26/21), which also found no gender differences in FPl engagement during emotional control (Tyborowska et al., 2016). Together, these results suggest that the observed differences in lPFC subregion recruitment are more likely attributable to individual differences in anxiety rather than gender.

JNeurosci Accepted Manuscript

## DISCUSSION (1362/1500)

This study demonstrates that in-phase dual-site tACS, targeted at facilitating endogenous theta-gamma phase-amplitude coupling between lPFC and SMC, enhances control over emotional action tendencies in highly socially anxious individuals. The main finding is that dual-site tACS effects, previously reported to improve control over automatic approach-avoidance tendencies in non-anxious participants (Bramson et al., 2020a), generalize to a clinically relevant population with altered control over daily-life social-emotional behavior (LSAS $\geq$ 30) (Mennin et al., 2002; Roelofs et al., 2009b; van Peer et al., 2009). Furthermore, this study shows that the dual-site tACS intervention in high-anxious males and females evokes effects in a different prefrontal territory (dlPFC) than in non-anxious males (FPl) (Bramson et al., 2020a). This observation fits the recently reported shift in the prefrontal circuit implementing emotional action control from FPl (non-anxious participants) to dlPFC (high-anxious participants) (Bramson et al., 2023). The current study demonstrates the possibility of improving emotional action control using dual-site tACS in high-anxious individuals via the facilitation of endogenous long-range phase-amplitude coupling. This finding extends our mechanistic understanding of approach-avoidance control in social anxiety and introduces rhythmic synchronization between dlPFC and SMC as a novel therapeutic tool.

### dlPFC-SMC phase-amplitude coupling supports emotional action control in social anxiety

This dual-site tACS intervention builds on prior studies that have demonstrated the significance of endogenous lPFC-SMC theta-gamma coupling in controlling automatic emotional action tendencies and in facilitating the implementation of alternative goal-directed actions (Bramson et al., 2018, 2020a). In this study, in-phase dual-site tACS could enhance interregional synchronization of neuronal excitability periods, biasing action selection in SMC according to valence-incongruent action goals in dlPFC (Voytek et al., 2015; Bramson et al., 2018; Weber et al., 2024). In one important detail, this putative mechanism differs from what has been observed in healthy individuals, where prefrontal control emerged from FPl (Bramson et al., 2020a) rather than dlPFC (this study). This difference is important for understanding the scope and the mechanism of the dual-site tACS intervention in social anxiety. Namely, FPl is a region that can flexibly integrate valence signals with approach-avoid action selection, allowing FPl to orchestrate goal-directed control over automatic emotional action tendencies (Bramson et al., 2020b; Lapate et al., 2022). However, FPl is overexcitable in high-anxious individuals (Bramson et al., 2023), and the evidence suggests dlPFC compensates for FPl when control over emotional actions is required (Bramson et al., 2023; Zhuang et al., 2025). In contrast with integrated valence-action goal representations observed in FPl, action goal representations in dlPFC are not modulated by

JNeurosci Accepted Manuscript

valence (Lapate et al., 2022), consistent with relatively sparse mono-synaptic connections from amygdala to dlPFC (Petrides and Pandya, 1999; Folloni et al., 2019). In fact, dlPFC engagement could dampen amygdala processing via strong indirect projections to the ventromedial subgenual cingulate area 25 (Joyce et al., 2020, 2023), thereby providing a candidate mechanism for gating the contribution of emotional afferences to cognitive control (Berboth and Morawetz, 2021). Thus, the dlPFC can implement rule-based actions with minimal interference from emotional valence signals even in high anxiety, when emotional signals would saturate an already overexcitable FPl (Bramson et al., 2023). However, this may come at a cost: dlPFC-based emotional action control might be limited when emotional challenges co-occur with demands for cognitive control, e.g. during real-life situations. Accordingly, high-anxious individuals show reduced dlPFC efficiency during cognitive control compared to non-anxious individuals (Eysenck et al., 2022). It remains to be seen whether dual-site tACS in socially-anxious individuals can enhance dlPFC coordination with SMC and remain behaviorally effective even in the presence of multiple cognitive control demands.

**tACS target engagement in dlPFC scales with trait anxiety**

The current study shows that the application of in-phase dual-site tACS results in behavioral effects proportional to BOLD signal evoked over dlPFC across tACS conditions, i.e., dependent on local target engagement. We also observe that individuals with higher trait anxiety exhibit more robust dlPFC responses to the tACS intervention. This finding corresponds to the observation that trait anxiety is associated with an anatomical shift of prefrontal emotional action control, from FPl to dlPFC (Bramson et al., 2023; Zhuang et al., 2025). The link between tACS response and trait anxiety signals that sub-optimal endogenous synchronization could underlie reduced emotion control performance in anxiety. Namely, the most robust effects of tACS are expected when weak endogenous oscillations can be facilitated (Krause et al., 2022), and in-phase dual-site tACS is expected to improve long-range communication by reducing noise within hypo-synchronized circuits (Wischnewski et al., 2023). Specifically, we suggest that trait anxiety might index individual levels of neural noise within the dlPFC-SMC circuit during emotional action control, a prediction that could be tested by measuring electrophysiological activity during emotional action control in high-anxious individuals (Bramson et al., 2018). This distinction may be important for clinical translation, as it suggests that direct neural readouts (e.g., concurrent fMRI or electrophysiology) currently provide a more specific proxy for stimulation engagement than trait measures alone.

**Interpretational issues and future directions**

JNeurosci Accepted Manuscript

It could be argued that the current findings are limited by the lack of electrophysiological observations of the consequences of tACS. In fact, the manipulation of dual-site tACS phase angle (in-phase *versus* anti-phase) enables us to relate the tACS effects to phase-specific changes in long-range phase-amplitude coupling, and exclude general changes in lPFC or SMC excitability. The phase manipulation provides the additional benefit of fully matching peripheral effects between in-phase and anti-phase stimulation, thereby ruling out alternative explanations related to transcutaneous entrainment or retinal stimulation (Schutter, 2016; Asamoah et al., 2019).

Our findings suggest that in-phase tACS reduces amygdala influence on action selection through network-level competition rather than direct prefrontal-amygdala modulation. We found no phase-dependent differences in dlPFC-amygdala functional connectivity, ruling out enhanced top-down regulation as the mechanism. Instead, the relationship between amygdala modulation and behavioral control weakened specifically as target engagement increased during in-phase—but not anti-phase—stimulation. This pattern indicates that enhanced dlPFC-SMC coupling strengthens goal-directed cortical control pathways that compete with amygdala-driven action tendencies at the level of motor output (Bramson et al., 2023). Future dedicated studies could test the changes in effective connectivity across the dlPFC-SMC-amygdala circuit as a function of cortical state.

In this study, phase-specific dual-site tACS improvements in emotional action control are related to target engagement, an indication of high inter-individual variation in the effects of dual-site tACS on emotional action control. This variation makes the tACS effects physiologically plausible, since tACS effects depends on the electric field induced in the brain (Krause et al., 2019; Johnson et al., 2020) and on the interaction with ongoing endogenous oscillations (Krause et al., 2022). Future studies could use individualized current flow models to optimize stimulation protocols and enhance targeting accuracy to achieve more consistent tACS effects (Grover et al., 2023). However, these models do not capture state-dependent effects in the neural response to stimulation (Bradley et al., 2022), which could be particularly relevant for translational efforts in which the neural mechanisms underlying the disorder are not fully understood. Inter-individual variation in tACS efficacy can be exploited to identify factors that could maximize intervention response, in particular when used to enhance the effectiveness of existing treatments. This can include improving the ability to control emotional behavior during exposure therapy to confront threatening situations and temporarily interrupt the cycle of persistent avoidance.

JNeurosci Accepted Manuscript

## CONCLUSION

Building non-invasive neuromodulation interventions that facilitate cognitive function presents a major neuroscientific challenge due to the need to identify and enhance the underlying endogenous neural dynamics. Translating mechanistically informed neuromodulation interventions from healthy individuals to clinical populations poses a further challenge due to an incomplete understanding of the neural mechanisms underlying psychiatric disorders. Here, we successfully translate a mechanistically informed dual-site tACS intervention (Bramson et al., 2018, 2020a) to a clinically relevant high-anxiety population that shows impairments in daily-life social-emotional behavior. The findings highlight the advantage of combining cognitive neuromodulation interventions with neuroimaging during the early stages of clinical translation. The advantage of this multi-modal approach is that it offers a better understanding of the intervention mechanism, leading to a more precise characterization of inter-individual variation in intervention response. The results provide insights into the role of phase-amplitude coupling between lPFC and SMC in emotion control over social approach-avoidance behavior and contribute to developing targeted clinical interventions for anxiety.

JNeurosci Accepted Manuscript

## REFERENCES


Algermissen J, Swart JC, Scheeringa R, Cools R, den Ouden HEM (2022) Striatal BOLD and midfrontal theta power express motivation for action. Cereb Cortex 32:2924–2942.

Amaral DG, Price JL (1984) Amygdalo-cortical projections in the monkey (Macaca fascicularis). Journal of Comparative Neurology 230:465–496.

Andersson JLR, Skare S, Ashburner J (2003) How to correct susceptibility distortions in spin-echo echo-planar images: application to diffusion tensor imaging. NeuroImage 20:870–888.

Anticevic A, Barch DM, Repovs G (2010) Resisting emotional interference: Brain regions facilitating working memory performance during negative distraction. Cognitive, Affective, & Behavioral Neuroscience 10:159–173.

Asamoah B, Khatoun A, Mc Laughlin M (2019) tACS motor system effects can be caused by transcutaneous stimulation of peripheral nerves. Nat Commun 10:266.

Bates D, Mächler M, Bolker B, Walker S (2015) Fitting Linear Mixed-Effects Models Using lme4. Journal of Statistical Software 67:1–48.

Beckmann CF, Smith SM (2004) Probabilistic independent component analysis for functional magnetic resonance imaging. IEEE Transactions on Medical Imaging 23:137–152.

Berboth S, Morawetz C (2021) Amygdala-prefrontal connectivity during emotion regulation: A meta-analysis of psychophysiological interactions. Neuropsychologia 153:107767.

Bradley C, Nydam AS, Dux PE, Mattingley JB (2022) State-dependent effects of neural stimulation on brain function and cognition. Nat Rev Neurosci 23:459–475.

Bramson B, den Ouden HE, Toni I, Roelofs K (2020a) Improving emotional-action control by targeting long-range phase-amplitude neuronal coupling Shackman A, Ivry RB, eds. eLife 9:e59600.

Bramson B, Folloni D, Verhagen L, Hartogsveld B, Mars RB, Toni I, Roelofs K (2020b) Human Lateral Frontal Pole Contributes to Control over Emotional Approach–Avoidance Actions. J Neurosci 40:2925–2934.

Bramson B, Jensen O, Toni I, Roelofs K (2018) Cortical Oscillatory Mechanisms Supporting the Control of Human Social–Emotional Actions. J Neurosci 38:5739–5749.

Bramson B, Meijer S, van Nuland A, Toni I, Roelofs K (2023) Anxious individuals shift emotion control from lateral frontal pole to dorsolateral prefrontal cortex. Nat Commun 14:4880.


JNeurosci Accepted Manuscript

Canolty RT, Knight RT (2010) The functional role of cross-frequency coupling. Trends in Cognitive Sciences 14:506–515.

Cohen N, Margulies DS, Ashkenazi S, Schaefer A, Taubert M, Henik A, Villringer A, Okon-Singer H (2016) Using executive control training to suppress amygdala reactivity to aversive information. NeuroImage 125:1022–1031.

Craske MG, Stein MB (2016) Anxiety. The Lancet 388:3048–3059.

Eklund A, Nichols TE, Knutsson H (2016) Cluster failure: Why fMRI inferences for spatial extent have inflated false-positive rates. Proceedings of the National Academy of Sciences 113:7900–7905.

Eysenck MW, Moser JS, Derakshan N, Hepsomali P, Allen P (2022) A neurocognitive account of attentional control theory: how does trait anxiety affect the brain's attentional networks? Cognition and Emotion 0:1–18.

Faul F, Erdfelder E, Lang A-G, Buchner A (2007) G*Power 3: A flexible statistical power analysis program for the social, behavioral, and biomedical sciences. Behavior Research Methods 39:175–191.

Folloni D, Sallet J, Khrapitchev AA, Sibson N, Verhagen L, Mars RB (2019) Dichotomous organization of amygdala/temporal-prefrontal bundles in both humans and monkeys Heilbronner S, Gold JI, Thiebaut de Schotten M, eds. eLife 8:e47175.

Ghashghaei HT, Hilgetag CC, Barbas H (2007) Sequence of information processing for emotions based on the anatomic dialogue between prefrontal cortex and amygdala. NeuroImage 34:905–923.

Griffanti L, Douaud G, Bijsterbosch J, Evangelisti S, Alfaro-Almagro F, Glasser MF, Duff EP, Fitzgibbon S, Westphal R, Carone D, Beckmann CF, Smith SM (2017) Hand classification of fMRI ICA noise components. NeuroImage 154:188–205.

Grover S, Fayzullina R, Bullard BM, Levina V, Reinhart RMG (2023) A meta-analysis suggests that tACS improves cognition in healthy, aging, and psychiatric populations. Science Translational Medicine 15:eabo2044.

Grover S, Wen W, Viswanathan V, Gill CT, Reinhart RMG (2022) Long-lasting, dissociable improvements in working memory and long-term memory in older adults with repetitive neuromodulation. Nat Neurosci 25:1237–1246.

Heuer K, Rinck M, Becker ES (2007) Avoidance of emotional facial expressions in social anxiety: The Approach–Avoidance Task. Behaviour Research and Therapy 45:2990–3001.

Jenkinson M, Bannister P, Brady M, Smith S (2002) Improved Optimization for the Robust and Accurate Linear Registration and Motion Correction of Brain Images. NeuroImage 17:825–841.

JNeurosci Accepted Manuscript

Jenkinson M, Beckmann CF, Behrens TEJ, Woolrich MW, Smith SM (2012) FSL. NeuroImage 62:782–790.

Johnson L, Alekseichuk I, Krieg J, Doyle A, Yu Y, Vitek J, Johnson M, Opitz A (2020) Dose-dependent effects of transcranial alternating current stimulation on spike timing in awake nonhuman primates. Science Advances 6:eaaz2747.

Joyce MKP, García-Cabezas MÁ, John YJ, Barbas H (2020) Serial Prefrontal Pathways Are Positioned to Balance Cognition and Emotion in Primates. J Neurosci 40:8306–8328.

Joyce MKP, Wang J, Barbas H (2023) Subgenual and Hippocampal Pathways in Amygdala Are Set to Balance Affect and Context Processing. J Neurosci 43:3061–3080.

Kaldewaij R, Koch SBJ, Hashemi MM, Zhang W, Klumpers F, Roelofs K (2021) Anterior prefrontal brain activity during emotion control predicts resilience to post-traumatic stress symptoms. Nat Hum Behav 5:1055–1064.

Kanske P, Heissler J, Schönfelder S, Bongers A, Wessa M (2011) How to Regulate Emotion? Neural Networks for Reappraisal and Distraction. Cerebral Cortex 21:1379–1388.

Koch SBJ, Mars RB, Toni I, Roelofs K (2018) Emotional control, reappraised. Neuroscience & Biobehavioral Reviews 95:528–534.

Krause MR, Vieira PG, Csorba BA, Pilly PK, Pack CC (2019) Transcranial alternating current stimulation entrains single-neuron activity in the primate brain. Proceedings of the National Academy of Sciences 116:5747–5755.

Krause MR, Vieira PG, Thivierge J-P, Pack CC (2022) Brain stimulation competes with ongoing oscillations for control of spike timing in the primate brain. PLOS Biology 20:e3001650.

Lapate RC, Ballard IC, Heckner MK, D'Esposito M (2022) Emotional Context Sculpts Action Goal Representations in the Lateral Frontal Pole. J Neurosci 42:1529–1541.

Leung LS, Yim CYC (2025) Inhibitory Postsynaptic Potentials Participate in Intracellular and Extracellular Theta Rhythms in the Hippocampus: A Personal Narrative. Hippocampus 35:e23660.

Lovibond PF, Mitchell CJ, Minard E, Brady A, Menzies RG (2009) Safety behaviours preserve threat beliefs: Protection from extinction of human fear conditioning by an avoidance response. Behaviour Research and Therapy 47:716–720.

Mennin DS, Fresco DM, Heimberg RG, Schneier FR, Davies SO, Liebowitz MR (2002) Screening for social anxiety disorder in the clinical setting: using the Liebowitz Social Anxiety Scale. J Anxiety Disord 16:661–673.

JNeurosci Accepted Manuscript

Morecraft RJ, McNeal DW, Stilwell-Morecraft KS, Gedney M, Ge J, Schroeder CM, van Hoesen GW (2007) Amygdala interconnections with the cingulate motor cortex in the rhesus monkey. Journal of Comparative Neurology 500:134–165.

Neubert F-X, Mars RB, Thomas AG, Sallet J, Rushworth MFS (2014) Comparison of Human Ventral Frontal Cortex Areas for Cognitive Control and Language with Areas in Monkey Frontal Cortex. Neuron 81:700–713.

Opitz A, Paulus W, Will S, Antunes A, Thielscher A (2015) Determinants of the electric field during transcranial direct current stimulation. NeuroImage 109:140–150.

O'Reilly JX, Woolrich MW, Behrens TEJ, Smith SM, Johansen-Berg H (2012) Tools of the trade: psychophysiological interactions and functional connectivity. Soc Cogn Affect Neurosci 7:604–609.

Petrides M, Pandya DN (1999) Dorsolateral prefrontal cortex: comparative cytoarchitectonic analysis in the human and the macaque brain and corticocortical connection patterns. European Journal of Neuroscience 11:1011–1036.

Phaf RH, Mohr SE, Rotteveel M, Wicherts JM (2014) Approach, avoidance, and affect: a meta-analysis of approach-avoidance tendencies in manual reaction time tasks. Frontiers in Psychology 5 Available at: https://www.frontiersin.org/articles/10.3389/fpsyg.2014.00378 [Accessed April 17, 2023].

Pittig A, Alpers GW, Niles AN, Craske MG (2015) Avoidant decision-making in social anxiety disorder: A laboratory task linked to in vivo anxiety and treatment outcome. Behaviour Research and Therapy 73:96–103.

Polanía R, Nitsche MA, Korman C, Batsikadze G, Paulus W (2012) The Importance of Timing in Segregated Theta Phase-Coupling for Cognitive Performance. Current Biology 22:1314–1318.

Preisig BC, Riecke L, Sjerps MJ, Kösem A, Kop BR, Bramson B, Hagoort P, Hervais-Adelman A (2021) Selective modulation of interhemispheric connectivity by transcranial alternating current stimulation influences binaural integration. Proceedings of the National Academy of Sciences 118:e2015488118.

Rattel JA, Miedl SF, Blechert J, Wilhelm FH (2017) Higher threat avoidance costs reduce avoidance behaviour which in turn promotes fear extinction in humans. Behaviour Research and Therapy 96:37–46.

Reinhart RMG, Nguyen JA (2019) Working memory revived in older adults by synchronizing rhythmic brain circuits. Nat Neurosci 22:820–827.

Roelofs K, Minelli A, Mars RB, van Peer J, Toni I (2009a) On the neural control of social emotional behavior. Social Cognitive and Affective Neuroscience 4:50–58.

JNeurosci Accepted Manuscript

Roelofs K, van Peer J, Berretty E, Jong P de, Spinhoven P, Elzinga BM (2009b) Hypothalamus–Pituitary–Adrenal Axis Hyperresponsiveness Is Associated with Increased Social Avoidance Behavior in Social Phobia. Biological Psychiatry 65:336–343.

Saturnino GB, Madsen KH, Siebner HR, Thielscher A (2017) How to target inter-regional phase synchronization with dual-site Transcranial Alternating Current Stimulation. NeuroImage 163:68–80.

Scheeringa R, Fries P, Petersson K-M, Oostenveld R, Grothe I, Norris DG, Hagoort P, Bastiaansen MCM (2011) Neuronal Dynamics Underlying High- and Low-Frequency EEG Oscillations Contribute Independently to the Human BOLD Signal. Neuron 69:572–583.

Schutter DJLG (2016) Cutaneous retinal activation and neural entrainment in transcranial alternating current stimulation: A systematic review. NeuroImage 140:83–88.

Smith SM, Nichols TE (2009) Threshold-free cluster enhancement: Addressing problems of smoothing, threshold dependence and localisation in cluster inference. NeuroImage 44:83–98.

Thielscher A, Antunes A, Saturnino GB (2015) Field modeling for transcranial magnetic stimulation: A useful tool to understand the physiological effects of TMS? In: 2015 37th Annual International Conference of the IEEE Engineering in Medicine and Biology Society (EMBC), pp 222–225.

Tyborowska A, Volman I, Smeekens S, Toni I, Roelofs K (2016) Testosterone during Puberty Shifts Emotional Control from Pulvinar to Anterior Prefrontal Cortex. J Neurosci 36:6156–6164.

van Peer JM, Spinhoven P, Dijk JG van, Roelofs K (2009) Cortisol-induced enhancement of emotional face processing in social phobia depends on symptom severity and motivational context. Biological Psychology 81:123–130.

Violante IR, Li LM, Carmichael DW, Lorenz R, Leech R, Hampshire A, Rothwell JC, Sharp DJ (2017) Externally induced frontoparietal synchronization modulates network dynamics and enhances working memory performance Hamilton R, ed. eLife 6:e22001.

Volman I, Borries AKL von, Bulten BH, Verkes RJ, Toni I, Roelofs K (2016) Testosterone Modulates Altered Prefrontal Control of Emotional Actions in Psychopathic Offenders. eNeuro 3 Available at: https://www.eneuro.org/content/3/1/ENEURO.0107-15.2016 [Accessed March 19, 2025].

Volman I, Roelofs K, Koch S, Verhagen L, Toni I (2011) Anterior Prefrontal Cortex Inhibition Impairs Control over Social Emotional Actions. Current Biology 21:1766–1770.

JNeurosci Accepted Manuscript

Volman I, Verhagen L, Ouden HEM den, Fernández G, Rijpkema M, Franke B, Toni I, Roelofs K (2013) Reduced Serotonin Transporter Availability Decreases Prefrontal Control of the Amygdala. J Neurosci 33:8974–8979.

Voytek B, Kayser AS, Badre D, Fegen D, Chang EF, Crone NE, Parvizi J, Knight RT, D'Esposito M (2015) Oscillatory dynamics coordinating human frontal networks in support of goal maintenance. Nat Neurosci 18:1318–1324.

Weber J, Solbakk A-K, Blenkmann AO, Llorens A, Funderud I, Leske S, Larsson PG, Ivanovic J, Knight RT, Endestad T, Helfrich RF (2024) Ramping dynamics and theta oscillations reflect dissociable signatures during rule-guided human behavior. Nat Commun 15:637.

Wischnewski M, Alekseichuk I, Opitz A (2023) Neurocognitive, physiological, and biophysical effects of transcranial alternating current stimulation. Trends in Cognitive Sciences 27:189–205.

Woolrich M (2008) Robust group analysis using outlier inference. NeuroImage 41:286–301.

Yu S, Stock A-K, Münchau A, Frings C, Beste C (2023) Neurophysiological principles of inhibitory control processes during cognitive flexibility. Cereb Cortex 33:6656–6666.

Zhuang Q, Yao S, Xu L, Chen S, Li J, Zheng X, Fu M, Kendrick KM, Becker B (2025) A functional anatomical shift from the lateral frontal pole to dorsolateral prefrontal cortex in emotion action control underpins elevated levels of anxiety: partial replication and generalization of Bramson et al., 2023. Psychoradiology 5:kkaf009.

JNeurosci Accepted Manuscript

## FIGURE LEGENDS

***Figure 1. Behavioral and BOLD fMRI effects related to control over emotional action tendencies. (A) Sample distribution of self-reported Liebowitz Social Anxiety Scale (LSAS) scores.*** *The black dashed line marks an LSAS score of 30, used to select socially anxious participants. This cut-off balances specificity and sensitivity in detecting heightened social anxiety* (Mennin et al., 2002). ***(B) Conceptual visualization of the approach-avoidance task performed during concurrent dual-site tACS and fMRI****. In affect-congruent conditions, participants were instructed to pull the joystick towards them in response to a happy face and push it away from them in response to an angry face. In contrast, the affect-incongruent condition requires participants to override automatic emotional action tendencies to avoid angry and approach happy faces. Therefore, in this condition, participants were instructed to pull the joystick towards them in response to an angry face and push it away in response to a happy face.* ***(C) Behavioral congruency-effects in the baseline sham stimulation condition of the task.*** *Participants made more errors when overriding their automatic emotional action tendencies in the affect-incongruent condition (orange circles) as compared to making affect-congruent responses (blue circles). Black-filled diamonds represent mean values, and standard errors of the mean are shown with black lines.* ***(D) Task-fMRI congruency-related effects across tACS stimulation conditions*** *(incongruent > congruent; cluster-level inferences corrected for multiple comparisons). Stronger BOLD signals were observed in prefrontal- and parietal areas when automatic emotional action tendencies needed to be overridden, while amygdala-hippocampal and medial-orbitofrontal areas showed weaker BOLD signals.*

***Figure 2. Dual-site phase-amplitude coupled tACS modulates endogenous inter-regional coupling between stimulation targets. (A) Modeled current density distribution at cortical targets.*** *Two sets of concentric ring electrodes were placed over the right lPFC and left SMC. The current density model shows the spatial distribution of the electric field magnitude evoked by the high-definition montage at both cortical targets.* ***(B) Dual-site phase-locked tACS manipulations.*** *The stimulation conditions underwent a pseudo-random alternation throughout the experiment between active in-phase tACS (green), active control anti-phase tACS (brown), and baseline sham (black). Specifically, 75 Hz stimulation was administered over the SMC and its amplitude modulated by the phase of a 6 Hz stimulation over the lPFC. Modulation was either in-phase or anti-phase with the peaks of the 6 Hz lPFC stimulation. While both in-phase and anti-phase tACS may influence local target excitability, in-phase tACS is specifically designed to enhance endogenous phase-amplitude coupling between the dlPFC and SMC, a mechanism*

JNeurosci Accepted Manuscript

*associated with successful emotional action control* (Bramson et al., 2018, 2020a)*. The baseline sham condition involved a brief 10-second initial stimulation that was discontinued before the start of the first trial.* ***(C) tACS-phase effect on congruency-related dlPFC-SMC coupling.*** *In-phase vs. anti-phase tACS selectively increased congruency-related functional coupling between dlPFC (seed) and SMC (target) stimulation areas (in-phase > anti-phase * incongruent > congruent), confirming the effectiveness of the tACS-phase manipulation in modulating inter-regional functional connectivity supporting emotional action control.*

***Figure 3. Phase- and target engagement-specific effects of dual-site tACS on emotional action control in social anxiety. (A) In-phase tACS facilitation of emotional action control is engagement dependent.*** *Participants who exhibited stronger inhibitory theta-band stimulation responses in dlPFC, as evidenced by a decrease in BOLD signal* (Scheeringa et al., 2011; Bramson et al., 2020a)*, demonstrated improved control over emotional actions (i.e., a reduced congruency effect) during in-phase tACS (green) compared to anti-phase tACS (brown). Black lines represent the fitted linear trend, with the shaded area indicating the associated 95% confidence interval.* ***(B) tACS-engagement scales with trait anxiety.*** *Concurrent tACS-fMRI BOLD signal changes across the in-phase and anti-phase tACS conditions (tACS engagement: tACS > sham) correlated with trait anxiety, indicating a stronger inhibitory dlPFC response in individuals with higher trait anxiety levels. To illustrate this relationship, we included a scatterplot depicting the association between trait anxiety scores and tACS-engagement values extracted from the maximum Z-value location within dlPFC.* ***(C) In-phase tACS improves general behavioral performance independent of tACS engagement.*** *In-phase (green panel) vs. anti-phase tACS (brown panel) selectively enhanced response accuracy across congruent (blue) and incongruent (orange) conditions compared to sham. Bar plots represent mean and standard error of the mean for each condition, with individual participant means indicated by grey dots.* ***(D) In-phase tACS of dlPFC-SMC coupling modulates amygdala contribution to valence-based action selection independent of tACS engagement.*** *Left: In the in-phase tACS condition, the right amygdala exhibited negative congruency-related BOLD signal (incongruent > congruent; cluster-level inferences corrected for multiple comparisons). White outlines indicate the anatomical bilateral amygdala mask used for extracting beta parameter estimates. Right: In-phase tACS (green panel) increased congruency-related amygdala modulation compared to anti-phase tACS (brown panel).*

***Figure 4. In-phase tACS may reduce amygdala influence on action selection through enhanced goal-directed cortical control. (A) Amygdala modulation relates to behavioral***

Neurosci Accepted Manuscript

***control in both tACS-phase conditions**. Relationship between amygdala congruency-related BOLD modulation (incongruent > congruent) and behavioral congruency effect (error rate: incongruent - congruent) for anti-phase (brown, left panel) and in-phase (green, right panel) tACS conditions. Negative correlations indicate that stronger amygdala modulation associates with better control over emotional action tendencies in both conditions (anti-phase: Spearman's $\rho_{(47)}$ = -0.30, p = 0.0400; in-phase: Spearman's $\rho_{(47)}$ = -0.32, p = 0.0277). Lines represent fitted linear trends with 95% confidence intervals shown as shaded areas. **(B) Target engagement modulates the amygdala-behavior relationship during in-phase but not anti-phase tACS**. Coupling between amygdala modulation and behavioral control varies as a function of target engagement (dlPFC BOLD response to tACS) across low (-1 SD), mean, and high (+1 SD) engagement levels. In-phase tACS (green lines) shows systematic weakening of the amygdala-behavior coupling as target engagement increases, with phase differences between conditions most pronounced at high engagement (b = -0.53, $t_{(78)}$ = -2.37, p = 0.0188). In contrast, anti-phase tACS (brown lines) shows stable amygdala-behavior coupling across all engagement levels. Lines represent predicted slopes from the mixed-effects model, with shaded areas indicating 95% CIs.*

JNeurosci Accepted Manuscript

974 **TABLE LEGEND**

975

976 ***Table 1.*** *Group-level effects in the whole-brain BOLD-GLM analysis were assessed using FSL's*
977 *FLAME 1 mixed-effects model with automatic outlier de-weighting. Cluster-level inferences were*
978 *family-wise error-corrected, applying a cluster-forming threshold of $|Z| > 2.3$ and $p < 0.05$.*

979

JNeurosci Accepted Manuscript

| contrast | # | Harvard-Oxford structural atlas brain region | cluster size voxels | MNI peak coordinates x | y | z | max. *Z*-value | corrected *p* |
|---|---|---|---|---|---|---|---|---|
| *incongruent > congruent* | 1 | precuneus,<br>middle temporal gyrus,<br>supramarginal gyrus,<br>angular gyrus,<br>posterior cingulate gyrus,<br>cuneal cortex,<br>lateral occipital cortex,<br>superior parietal lobule,<br>left precentral gyrus,<br>left postcentral gyrus | 7059 | 14 | -70 | 36 | 5.03 | 3.43e-27 |
| | 2 | right frontal pole,<br>right middle frontal gyrus | 1099 | 30 | 36 | 38 | 4.61 | 7.15e-07 |
| | 3 | lingual gyrus,<br>right intracalcarine cortex,<br>right temporal occipital fusiform cortex,<br>right precuneus cortex | 814 | 16 | -74 | -4 | 3.70 | 2.22e-05 |
| | 4 | right paracingulate gyrus,<br>right anterior cingulate gyrus | 326 | 8 | 32 | 28 | 3.71 | 0.027 |
| *congruent > incongruent* | 1 | left temporal pole,<br>left amygdala,<br>left hippocampus,<br>left anterior parahippocampal gyrus,<br>left temporal fusiform cortex | 1376 | -42 | 16 | -36 | 4.86 | 5.96e-08 |
| | 2 | right amygdala, | 1028 | 38 | -4 | -20 | 3.98 | 1.61e-06 |

JNeurosci Accepted Manuscript

| | | | | | | | |
|---|---|---|---|---|---|---|---|
| | right hippocampus,<br>right anterior parahippocampal gyrus,<br>right temporal pole,<br>right subcallosal cortex,<br>right temporal fusiform cortex | | | | | | |
| 3 | frontal medial cortex,<br>frontal pole | 642 | -8 | 34 | -14 | 3.99 | 0.000217 |
| 4 | temporal occipital fusiform cortex,<br>inferior temporal gyrus,<br>lateral occipital cortex | 515 | 40 | -42 | -18 | 4.16 | 0.00134 |
| 5 | right frontal orbital cortex,<br>right frontal pole | 470 | 24 | 28 | -14 | 4.06 | 0.00264 |
| 6 | left frontal orbital cortex,<br>left frontal pole | 470 | -40 | 28 | -14 | 4.05 | 0.00264 |

***Table 1. Significant congruency-related whole-brain BOLD activation clusters.***

JNeurosci Accepted Manuscript

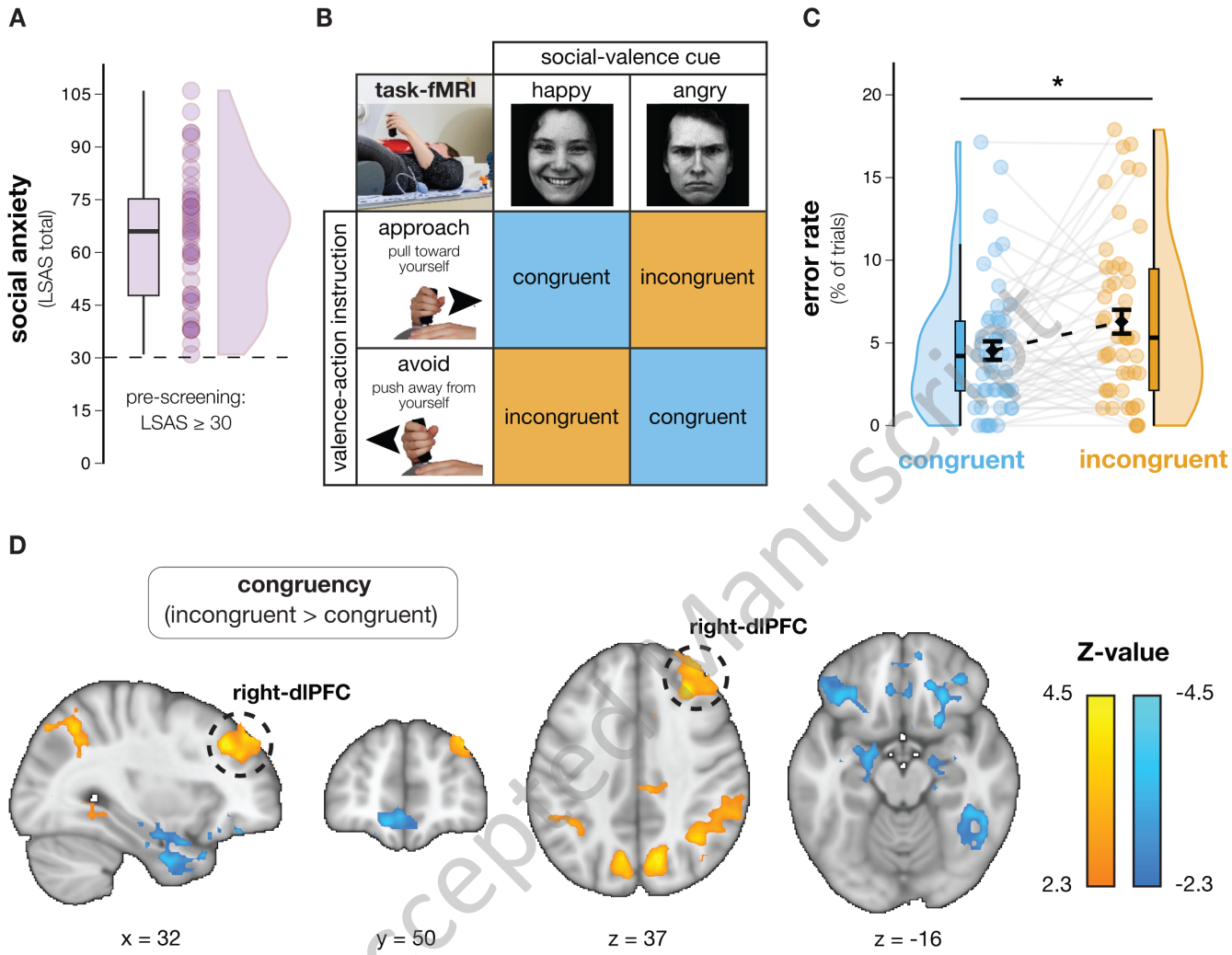


JNeurosci Accepted Manuscript

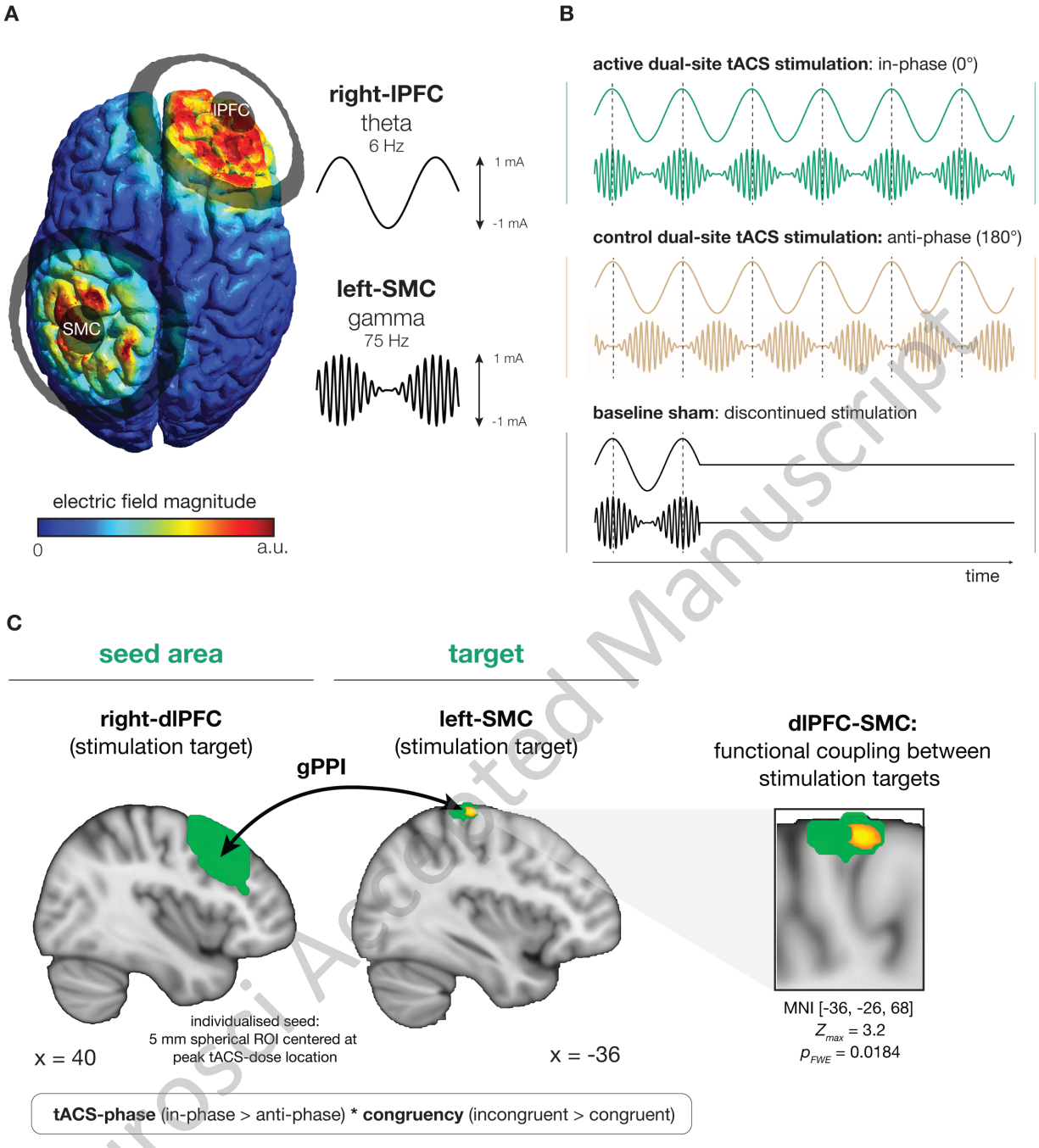


JNeurosci Accepted Manuscript

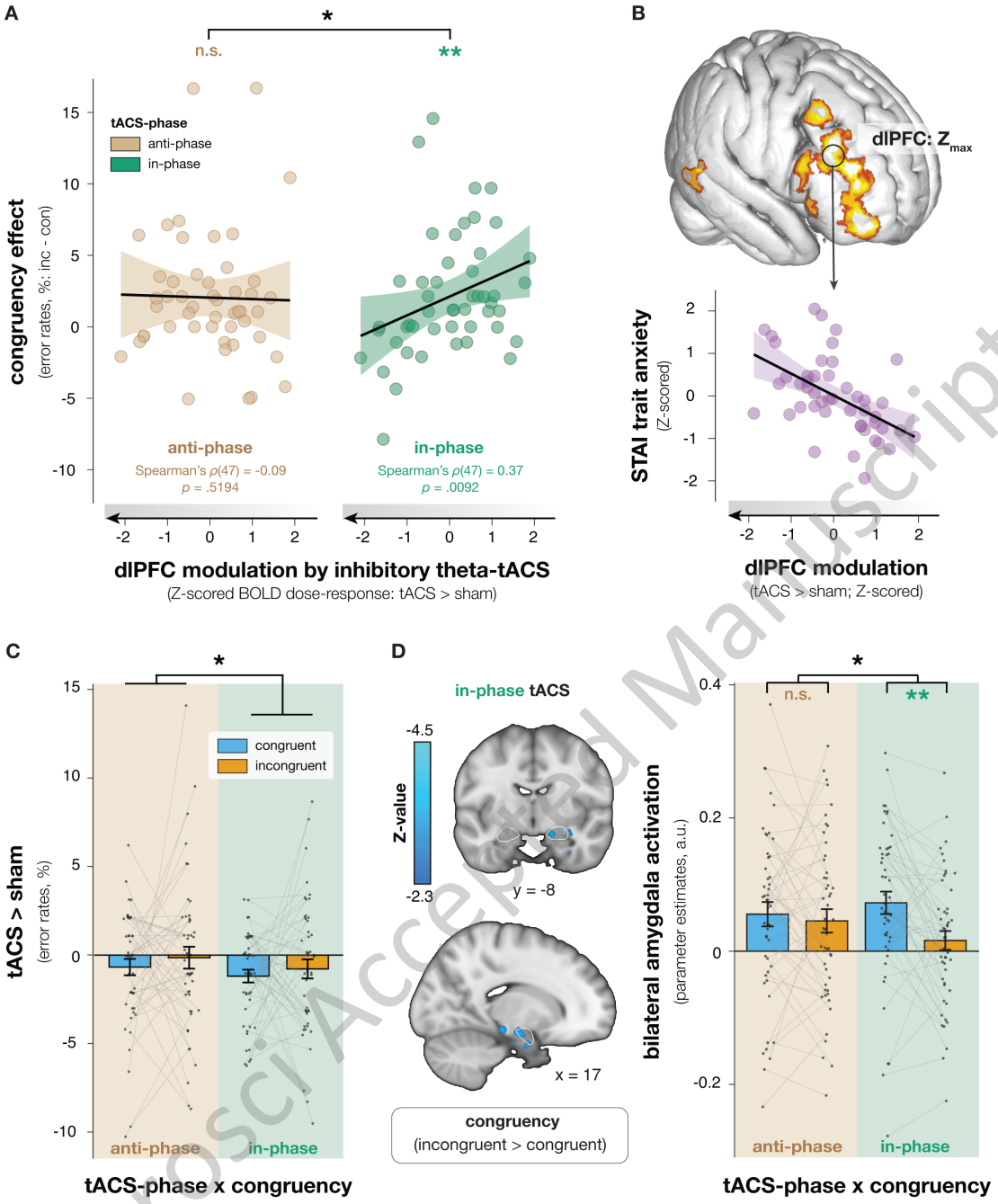


JNeurosci Accepted Manuscript

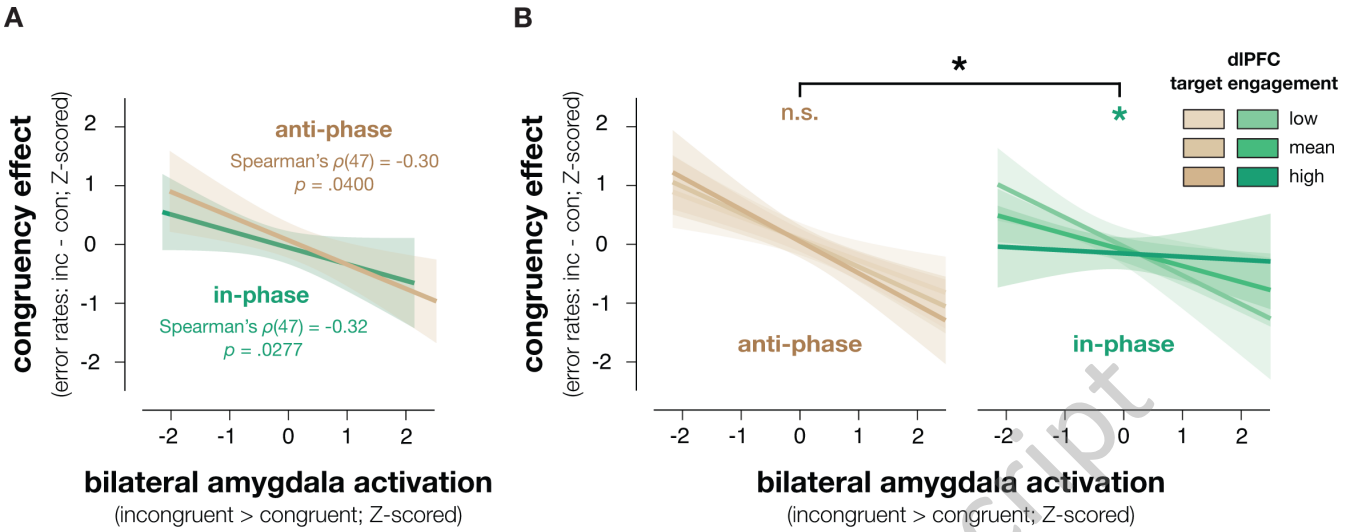


JNeurosci Accepted Manuscript